energies

MDPI

Article

Optimal Economic and Emission Dispatch of a Microgrid with a Combined Heat and Power System

Liangce He [1], Zhigang Lu [1,*], Lili Pan [2], Hao Zhao [3], Xueping Li [1] and Jiangfeng Zhang [4]

[1] Key Lab of Power Electronics for Energy Conservation and Motor Drive of Hebei Province, Yanshan University, Qinhuangdao 066004, Hebei, China; hlc@stumail.ysu.edu.cn (L.H.); lixueping@ysu.edu.cn (X.L.)
[2] Cangzhou Power Supply Branch, State Grid Hebei Electric Power Co., Ltd., Cangzhou 061000, Hebei, China; 18233587109@163.com
[3] China Energy Engineering Group, Tianjin Electric Power Design Institute Co., Ltd., Tianjin 300400, China; zhaohaoysu@163.com
[4] School of Electrical and Data Engineering, University of Technology Sydney, Sydney, NSW 2007, Australia; Jiangfeng.Zhang@uts.edu.au
* Correspondence: zhglu@ysu.edu.cn; Tel.: +86-0335-8387-565

Received: 28 December 2018; Accepted: 5 February 2019; Published: 14 February 2019

Abstract: With the rapid development of the new concept of energy internet, electric power systems often need to be investigated together with thermal energy systems. Additionally, to reduce pollution from gas emissions, it is very important to study the economic and emission dispatch of integrated electrical and heating systems. Hence, this paper proposes a multi-objective optimization dispatch model for a microgrid (MG) with a combined heat and power (CHP) system. This CHP-based MG system consists of a CHP unit, a wind turbine, a PV system, a fuel cell, an electric boiler, an electric storage, and a heat storage. It can exchange electricity with the distribution network and exchange heat with the district heating network. Minimum economic cost and minimum environmental cost are considered as the two objectives for the operation of this CHP-based MG system. To solve the two objective optimization problem, the multi-objective bacterial colony chemotaxis algorithm is utilized to obtain the Pareto optimal solution set, and the optimal solution is chosen by the Technique for Order of Preference by Similarity to Ideal Solution method. Finally, numerical case studies demonstrate the effectiveness of proposed model and method for the optimal economic and emission dispatch of the CHP-based MG system.

Keywords: combined heat and power system; economic and emission dispatch; microgrid; multi-objective optimization; energy internet

1. Introduction

With the wide concern on the gradual depletion and pollution emission of fossil fuels, renewable energy such as wind and solar has been significantly developed [1,2]. To effectively utilize renewable energy, microgrid (MG) technology has been intensively investigated, since an MG can integrate various distributed generations, energy storage units, load, and control devices together. In addition, the combined heat and power (CHP) system can provide both electricity and heat to users, and it has been widely applied in many MGs due to its high energy efficiency. Such a CHP-based MG system is composed of both electric and thermal energy sources, which is covered by the new concept of energy internet [3], where the efficient utilization of multiple energy resources is emphasized. Thus, the study of the CHP-based MG systems is significant for practical applications.

There are already a significant amount of studies on the design and operation of the CHP-based MG system. In [4], a sizing strategy of power sources and energy storage system is proposed for an

autonomy MG. A novel methodology is developed to offer a range of MG designs for an isolated community in [5], where each of them is optimal for a given consumption pattern. Different design options in building services are presented in [6] by using a fuel cell micro-CHP. In [7], an MG model is studied for planning the micro-CHP systems in agreement with the Portuguese energy legal framework, and thus it can design, evaluate, and optimize from the techno-economic point of view for any micro-CHP plant. In [8,9], the optimal sizing of an energy storage system and CHP units in an MG is obtained by the cost benefit analysis method. In [10], a promising energy supply chain network is proposed based on residential-scale micro-generation through micro-CHP systems. The interchange of electrical energy can take place among the members of this domestic MG, which is connected to the distribution network for potential power interchange. Considering the trade-off between total annual cost and electrical system unavailability, a mixed-integer linear programming (MILP) approach is proposed for the design of a neighborhood-based energy system [11]. Moreover, CHP-based MG systems can also include drinkable water and cooling system [12]. In [13], different energy storage options are considered in the design and management of a hybrid CHP-based MG system, and then the presented model is optimized by the particle swarm optimization (PSO) method. In [14], the optimal design and operation strategy of a trigeneration system is presented under both the stand-alone and grid-connected modes.

Extensive work has been done for the optimal operation of the CHP-based MG system. In [15,16], the optimal matching between the electric power source and electric load, and also the heat source and heat load, are considered within the CHP-based MG systems. In [17], an optimal dispatch model of a CHP-based MG system is proposed with heating, cooling, and electricity at the regional level, and a demand response (DR) mechanism is designed accordingly. In [18,19], the optimal energy management of different CHP-based MG systems is discussed to promote the energy exchange among buildings by utilizing various renewable energy resources. In [20], the building thermal inertia is discussed, and a feasible region method is presented for the optimization of a CHP-based MG system. In [21], a rolling horizon approach is introduced to deal with uncertainties of a CHP-based MG system associated to production and consumption. In [22], a new techno-economic model is proposed for a CHP-based MG system to investigate the business case under different combinations of services. Considering the coordination of fuel cell and CHP, an optimal economic dispatch model is studied for an industrial CHP-based MG system [23].

Furthermore, traditional optimization problems of the CHP-based MG system mainly target at the minimization of economic cost, then gradually environmental impact has also been considered along with the economic cost. In [24], greenhouse gas emission and energy consumption are both considered in the presented model of an industrial CHP-based MG system. Aiming to minimize the operation and emission costs, an optimization procedure is developed in [25] for the day-ahead scheduling of a CHP-based MG system. A probabilistic multi-objective optimization model of a CHP-based MG system is proposed in [26] considering operating cost and pollution emissions minimization under uncertain environment. However, most of the above research in [4–26] mainly considers electric power exchange with the distribution network, and thus the economic benefit and flexibility of CHP-based MG systems may be limited.

In view of the above problem, this paper establishes mathematical models for a CHP-based MG system including a CHP unit with a micro-turbine and a bromine chiller, a wind turbine, a photovoltaic (PV) system, a fuel cell, an electric boiler, an electric storage (ES) and a heat storage (HS). The CHP-based MG system is connected to both the distribution network and the district heating network, which makes the operation of the CHP-based MG system more flexible. To further analyze the presented CHP-based MG system, a multi-objective optimization model is proposed to minimize both the economic cost and environmental cost. Moreover, the multi-objective optimization model is a multidimensional, non-smooth, nonconvex, and nonlinear optimization problem, and thus an effective solution algorithm is needed. Multi-objective bacterial colony chemotaxis (MOBCC) algorithm is a new colony intelligence optimization algorithm [27]. This algorithm considers not only the chemotactic

strategy but also the communication between the colony members. MOBCC algorithm has been used to solve the economic emission dispatch (EED) problem, and the performance has been improved greatly against other algorithms [28,29]. It is gaining more attention due to its advantages of fast convergence and high precision for solving complex optimization problems. Hence, this paper uses MOBCC algorithm to solve the proposed multi-objective optimization model of the CHP-based MG system.

The major contributions of this paper are as follows.

(1) A flexible CHP-based MG system is presented by considering the energy exchange with both the distribution network and the district heating network.
(2) A multi-objective economic and emission dispatch model is proposed to study the flexible CHP-based MG system by considering the economic cost and environmental cost, and then it is solved by the MOBCC algorithm. After that, the Technique for Order of Preference by Similarity to Ideal Solution (TOPSIS) method [30] is adopted to choose the optimal decision solution for decision makers.

The remainder of the paper is organized as follows. Section 2 provides the description of the CHP-based MG system, and then the detailed mathematical models are presented; Section 3 proposes the multi-objective economic and emission dispatch model of the CHP-based MG system; Section 4 adopts the MOBCC algorithm and TOPSIS method to solve the optimization problem and to obtain the optimal decision solution, respectively. Finally, the main simulation results are discussed in Section 5 and the key conclusions are presented in Section 6.

2. System Description and Model Formulation

2.1. System Description

The structure and energy flow of the CHP-based MG System are shown in Figure 1. The CHP-based MG system includes a CHP unit, a wind turbine, a PV system, a fuel cell, an electric boiler, an electric storage, and a heat storage. Compared with the electric only MGs, this CHP-based MG system is able to exchange heat with district heating network through the heat supply pipeline.

To better describe the thermal energy system, the structure of the thermal energy system is shown in Figure 2. High temperature hot water is transferred from the heat pipe to the user through the radiator. Then the high temperature hot water turns into low temperature warm water, which goes back to the heat source through the return pipeline. The heat storage tank in the CHP-based MG system plays a role in decoupling the CHP unit into thermal part and electrical part. The electric boiler is expected to heat water during the period when the renewable energy generation is large and the electric load is low. Additionally, if the heat power output of the CHP unit is reduced, then the corresponding thermal demand of end users will be compensated by the electric boiler, which can use more renewable energy generation and save the fuel cost of the CHP unit. As the district heating network is connected to the CHP-based MG system, it can provide heat to meet the thermal load during the thermal load peak period. Meanwhile, when the CHP-based MG system has less thermal load, the excessive heat of the CHP-based MG system can be sold to the district heating network which will be transferred to users outside of this MG system. Note that the heat loss of the pipelines within the CHP-based MG system is negligible compared to the heat exchange loss between the CHP-based MG system and the district heating network, this is because the latter has longer pipe length and thus will be considered in this paper. More discussions on the heat loss and transport distance can be found in [6,11].

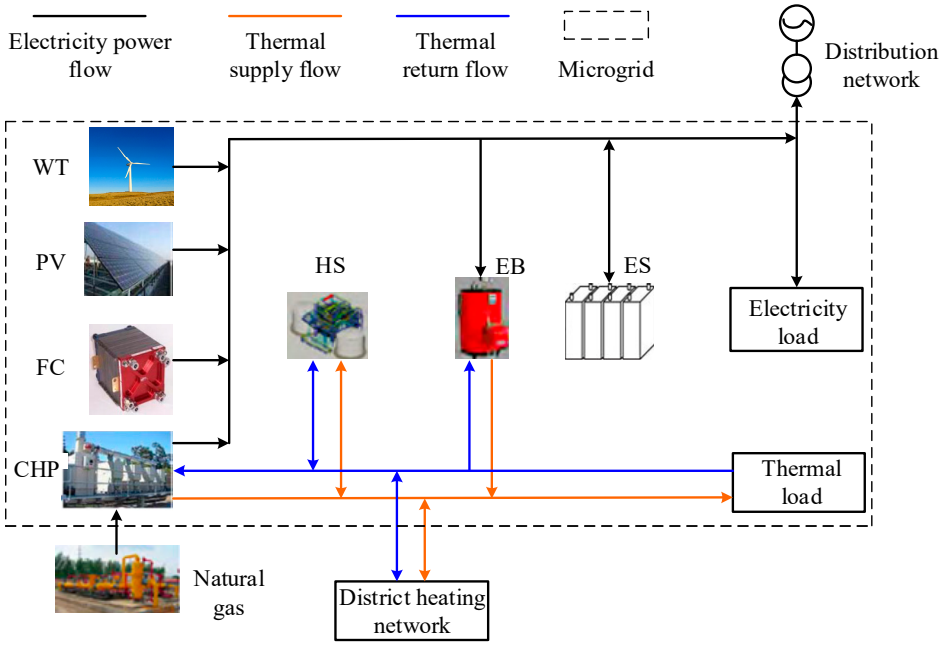

Figure 1. Structure and energy flow of CHP-based MG system.

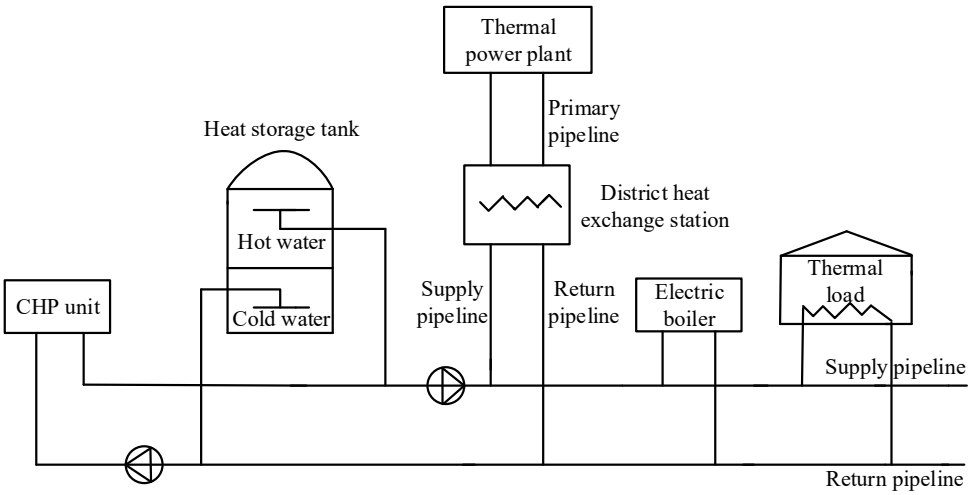

Figure 2. Structure of thermal energy system.

2.2. Model Formulation

2.2.1. CHP Unit

The CHP unit consists of a micro-turbine and a bromine chiller. The micro-turbine uses natural gas as fuel to generate electricity, and the relation between electricity and heat is

$$Q_{\mathrm{MT}}(t) = \frac{P_{\mathrm{MT}}(t)(1-\eta_{\mathrm{MT}}(t)-\eta_{\mathrm{HL}})}{\eta_{\mathrm{MT}}(t)} \tag{1}$$

Then the high temperature flue gas from the micro-turbine enters the bromine chiller to preheat water for the purpose of energy efficiency improvement.

$$Q_{\mathrm{MT,h}}(t) = Q_{\mathrm{MT}}(t)R_{\mathrm{MT}} \tag{2}$$

The fuel cost of micro-turbine is shown below.

$$C_{\mathrm{MT}}(t) = C_{\mathrm{NG}} \frac{P_{\mathrm{MT}}(t)\Delta t}{\eta_{\mathrm{MT}}(t) \times L_{\mathrm{HV}}} \tag{3}$$

The efficiency of micro-turbine can be calculated as [31]

$$\eta_{\mathrm{MT}}(t) = 0.0753\left(\frac{P_{\mathrm{MT}}(t)}{65}\right)^3 - 0.3095\left(\frac{P_{\mathrm{MT}}(t)}{65}\right)^2 + 0.4174\left(\frac{P_{\mathrm{MT}}(t)}{65}\right) + 0.1068 \tag{4}$$

2.2.2. Fuel Cell

A fuel cell is a power generation device that converts chemical energy stored in natural gas and methanol hydrogen-containing fuel into electricity. Because of its high efficiency of power generation, the heat loss is not considered. The relationship between fuel cost and power generation can be described below.

$$C_{\mathrm{FC}}(t) = C_{\mathrm{NG}} \frac{P_{\mathrm{FC}}(t)\Delta t}{\eta_{\mathrm{FC}}(t) \times L_{\mathrm{HV}}} \tag{5}$$

Similar to the micro-turbine, the efficiency of fuel cell can be expressed as [32]

$$\eta_{\mathrm{FC}}(t) = -0.0023 P_{\mathrm{FC}}(t) + 0.6735 \tag{6}$$

2.2.3. Electric Boiler

With the exception of the CHP unit, the electric boiler can convert electricity into heat to meet the heat load. The electric boiler model is shown as

$$Q_{\mathrm{EB}}(t) = P_{\mathrm{EB}}(t)\eta_{\mathrm{EB}} \tag{7}$$

2.2.4. Energy Storage System

Electric Storage

The lead–acid battery is installed in this CHP-based MG system as an electric storage device due to its low cost. The battery storage system can shift power consumption from one period to another, and thereby reduce the operational cost of the CHP-based MG system. The charging and discharging processes should meet the following requirement

$$E_{\mathrm{ES}}(t) = (1-\tau)E_{\mathrm{ES}}(t-1) + [P_{\mathrm{ES,ch}}(t)\eta_{\mathrm{ES,ch}} - \frac{P_{\mathrm{ES,dis}}(t)}{\eta_{\mathrm{ES,dis}}}]\Delta t \tag{8}$$

Heat Storage

As one of the most widely used heat storage devices, the heat storage tank is deployed in this CHP-based MG system as a heat storage device. The heat storage tank can alleviate the mismatch between the CHP energy supply and the electric and heat demand. It stores heat when thermal demand is low, while releases heat during the peak demand period. The heat storage model is similar to the electric storage model, and the expression is

$$H_{\mathrm{HS}}(t) = (1-\mu)H_{\mathrm{HS}}(t-1) + [Q_{\mathrm{HS,ch}}(t)\eta_{\mathrm{HS,ch}} - \frac{Q_{\mathrm{HS,dis}}(t)}{\eta_{\mathrm{HS,dis}}}]\Delta t \tag{9}$$

3. Multi-Objective Optimization Dispatch Model

3.1. Objective Functions

In this section, a multi-objective optimization dispatch model of the CHP-based MG system is established to minimize the economic cost and environmental cost. The economic cost C_1 can be expressed as (10), which includes the fuel costs of the micro-turbine and fuel cell defined in (3) and (5), the equipment operation and maintenance cost (11), the cost of the MG to exchange electric power with the distribution network (12), and the cost of the MG to exchange thermal power with the district heating network (13).

$$\min C_1 = \sum_{t=1}^{N_T} (C_{\mathrm{MT}}(t) + C_{\mathrm{FC}}(t) + C_{\mathrm{OM}}(t) + C_{\mathrm{EXE}}(t) + C_{\mathrm{EXH}}(t))\Delta t \tag{10}$$

$$C_{\mathrm{OM}}(t) = \sum_{i=1}^{N_M} K_{OM,i} P_i(t) \tag{11}$$

$$C_{\mathrm{EXE}}(t) = \frac{C_{\mathrm{E,buy}}(t) + C_{\mathrm{E,sell}}(t)}{2} P_{\mathrm{EXE}}(t) + \frac{C_{\mathrm{E,buy}}(t) - C_{\mathrm{E,sell}}(t)}{2} |P_{\mathrm{EXE}}(t)| \tag{12}$$

$$C_{\mathrm{EXH}}(t) = \frac{C_{\mathrm{H,buy}}(t) + C_{\mathrm{H,sell}}(t)}{2} Q_{\mathrm{EXH}}(t) + \frac{C_{\mathrm{H,buy}}(t) - C_{\mathrm{H,sell}}(t)}{2} |Q_{\mathrm{EXH}}(t)| \tag{13}$$

where N_M is equal to 6, and the index $i = 1, 2, 3, 4, 5, 6$ represents the micro-turbine, wind turbine, PV system, fuel cell, electric storage, and heat storage, respectively; $K_{\mathrm{OM}i}$ is the operation and maintenance cost per kW of unit i; $P_i(t)$ is the output power of unit i at time t. In (12)–(13), $P_{\mathrm{EXE}}(t)$ is the amount of exchanged electric power at time t, and a positive $P_{\mathrm{EXE}}(t)$ means that the MG buys electricity from power grid; $Q_{\mathrm{EXH}}(t)$ is the amount of exchanged thermal power at time t, and a positive $Q_{\mathrm{EXH}}(t)$ means that the MG buys heat from the district heating network.

The environmental cost C_2, namely the penalty fees of pollutant emission consisting of NO_X, SO_2 and CO_2, can be expressed as

$$\min C_2 = \sum_{t=1}^{N_T} \sum_{k=1}^{N_E} [C_k(\gamma_{MT,k} P_{MT}(t) + \gamma_{EXE,k} P_{EXE}(t)\alpha_{\mathrm{E}} + \gamma_{EXH,k} Q_{EXH}(t)\alpha_{\mathrm{H}})]\Delta t \tag{14}$$

where N_E is equal to 3, and the index k = 1, 2, 3 represents NO_X, SO_2 and CO_2 pollutant emission, respectively; $\alpha_{\mathrm{E}}, \alpha_{\mathrm{H}}$ are binary variables, α_{E} equals 1 for $P_{\mathrm{EXE}}(t) > 0$, and 0 otherwise; similarly, α_{H} equals 1 for $Q_{\mathrm{EXH}}(t) > 0$, and 0 otherwise.

3.2. Constraints

The dispatch model is subject to equality constraints of power and heat balance and inequality constraints of energy source operations, which are detailed below:

(1) Power balance constraints:

$$P_{\mathrm{MT}}(t) + P_{\mathrm{WT}}(t) + P_{\mathrm{PV}}(t) + P_{\mathrm{FC}}(t) + P_{\mathrm{ES,dis}}(t) - P_{\mathrm{ES,ch}}(t) + P_{\mathrm{EXE}}(t) = P_{\mathrm{L}}(t) + P_{\mathrm{EB}}(t) \tag{15}$$

(2) Heat balance constraints:

$$Q_{\mathrm{MT,h}}(t) + Q_{\mathrm{EB}}(t) + (1-\delta)Q_{\mathrm{EXH}}(t) + Q_{\mathrm{HS,dis}}(t) - Q_{\mathrm{HS,ch}}(t) = Q_{\mathrm{L}}(t) \tag{16}$$

where δ is the heat loss rate of heat exchange between the CHP-based MG system and the district heating network.

(3) Constraints of electric power exchange between MG and power grid:

$$P_{\mathrm{EXE,min}} \le P_{\mathrm{EXE}}(t) \le P_{\mathrm{EXE,max}} \tag{17}$$

where $P_{\mathrm{EXE,min}}$ is the minimum allowed electric power exchange with the tie line, and it is negative; $P_{\mathrm{EXE,max}}$ is the maximum allowed electric power exchange with the tie line, and it is positive.
(4) Constraints of heat power exchange between the CHP-based MG system and the district heating network:

$$Q_{\mathrm{EXH,min}} \le Q_{\mathrm{EXH}}(t) \le Q_{\mathrm{EXH,max}} \tag{18}$$

where $Q_{\mathrm{EXH,min}}$ is the minimum amount of exchanged heat power, and it is negative; $Q_{\mathrm{EXH,max}}$ is the maximum amount of exchanged heat power which is always positive.

(5) Power output constraints of PV system and wind turbine:

$$0 \le P_{\mathrm{PV}}(t) \le P_{\mathrm{PV}}^{\max} \tag{19}$$

$$0 \le P_{\mathrm{WT}}(t) \le P_{\mathrm{WT}}^{\max} \tag{20}$$

(6) Operating constraints of controllable units:

The micro-turbine, electric boiler and fuel cell are controllable units in the MG, thus they are subject to the relevant operational constraints, which include the upper and lower power limits (21) and ramp constraints (22).

$$P_{j\min}^{\mathrm{CU}} \le P_{j}^{\mathrm{CU}}(t) \le P_{j\max}^{\mathrm{CU}} \tag{21}$$

$$R_{j}^{\mathrm{down}}\Delta t \le P_{j}^{\mathrm{CU}}(t) - P_{j}^{\mathrm{CU}}(t-1) \le R_{j}^{\mathrm{up}}\Delta t \tag{22}$$

where $P_{j}^{\mathrm{CU}}(t)$ is the power output of controllable unit j, and j = 1,2,3 denotes the output of micro-turbine, electric boiler, and fuel cell at time t, respectively; $P_{j\min}^{\mathrm{CU}}$ and $P_{j\max}^{\mathrm{CU}}$ are the minimum power output and maximum power output of controllable unit j, respectively; R_{j}^{up} and R_{j}^{down} are the ramp up rate and ramp down rate of controllable unit j, respectively.

(7) Constraints of the energy storage system

As the electric storage model is similar to heat storage model, their constraints can be unified as energy storage system (ESS) constraints. ESS represents either electric storage or heat storage, and the following equations represent that both electric storage and heat storage satisfy these constraints.

$$\mathrm{SOC}_{\min} E_{\mathrm{ESS,max}} \le E_{\mathrm{ESS}}(t) \le \mathrm{SOC}_{\max} E_{\mathrm{ESS,max}} \tag{23}$$

$$-\gamma_{\mathrm{ESS,ch}} E_{\mathrm{ESS,max}} \le P_{\mathrm{ESS}}(t) \le \gamma_{\mathrm{ESS,dis}} E_{\mathrm{ESS,max}} \tag{24}$$

The ESSs are usually not allowed to be charged and discharged at the same time, and then the following constraint holds.

$$P_{\mathrm{ESS,ch}}(t) \cdot P_{\mathrm{ESS,dis}}(t) = 0 \tag{25}$$

Note the fact that the optimization procedure will tend to drive the final energy status of the ESS to be 0 if initially the ESS is empty. Therefore, to ensure a proper periodic operation, the initial amount of energy of the ESS is assumed to equal the energy at the final instant of the control period.

$$E_{\mathrm{ESS}}(0) = E_{\mathrm{ESS}}(N_T) \tag{26}$$

where $E_{\mathrm{ESS}}(0)$ is the initial energy of ESS at time 0; $E_{\mathrm{ESS}}(N_T)$ is the final energy of ESS at time N_T.

4. Solution Method

The objective of this model is to optimize both of the economic cost and environmental cost of the CHP-based MG system. It can be seen from Equations (3) and (4) that there is a complex nonlinear relation between decision variable electric power $P_{MT}(t)$ and power generation efficiency $\eta_{MT}(t)$. This is a multidimensional, non-smooth, nonconvex, and nonlinear multi-objective optimization model. The MOBCC algorithm [29] possesses better performance in terms of convergence to the Pareto set and maintains good diversity for non-dominated solutions for multi-objective optimization problem. Therefore, this paper uses the MOBCC algorithm to solve the model, and the flow chart of the solving process is shown in Figure 3.

Since there is a set of Pareto-optimal solutions obtained by MOBCC, the decision maker needs to select an optimal solution as the final scheduling result. The TOPSIS method [30] can set the weight according to the requirement of the decision maker, and the obtained final solution is close to the positive ideal solution and far away from the negative ideal solution. Thus, the optimal solution is selected by the TOPSIS method in this paper.

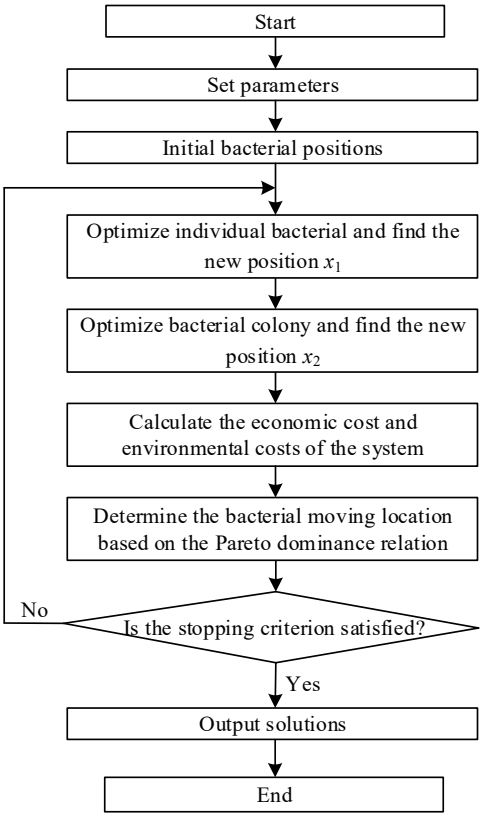

Figure 3. Flowchart of solving process.

5. Simulation Results

5.1. Parameters

In this section, the proposed economic and emission dispatch model is applied to the CHP-based MG system in Figures 1 and 2. The proposed model considers a 24-h scheduling cycle with a sampling period of one hour. A typical winter day of northern China is considered, and its predicted heat load, electric power load, the power outputs of WT and PV are shown in Figure 4. The operating parameters of the CHP-based MG system are shown in Table 1. The fixed supply heat price refers to [32]. The time-of-use (TOU) electricity price considered in this case study is a three-part tariff with detailed purchasing and selling price listed in Table 2. There are 8 h for the peak, 8 h for the valley,

and 8 h for the intermediate period. The specific parameters of ESS are shown in Table 3. In order to take advantage of ES and HS, and also to reduce the operational cost of the system, we set the minimum SOC (state of charge) of ES as initial SOC of ES, and the maximum SOC of HS as initial SOC of HS. The pollutant emission data and penalty standards are shown in Table 4, and other parameters used in the model are given in Table 5. For the MOBCC algorithm and TOPSIS method, the parameters are selected from [29,30].

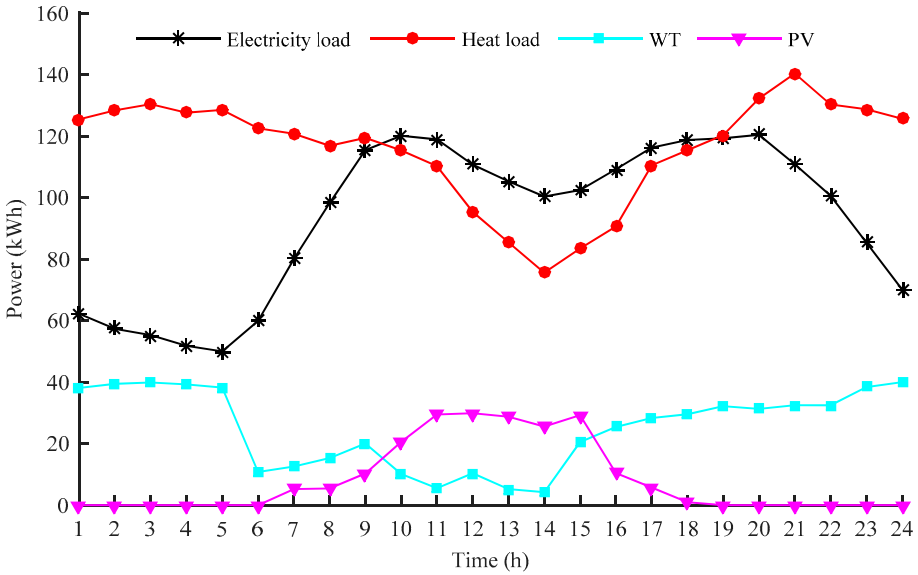

Figure 4. Forecast value of WT, PV, and load in a typical day in winter.

Table 1. Operating limits of CHP-based MG system.

Type	P_{min}/(kW)	P_{max}/(kW)	R^{down}/(kW/min)	R^{up}/(kW/min)	K_{OM}/($/kWh)
MT	15	65	5	10	0.0038
FC	5	40	2	2	0.0039
EB	0	50	/	/	0.0024
WT	0	40	/	/	0.0029
PV	0	30	/	/	0.0035
$P_{EXE}(t)$	−40	40	/	/	/
$Q_{EXH}(t)$	−40	40	/	/	/

Table 2. TOU price [33].

Period	Hours Covered	$C_{E,buy}(t)$/($/kWh)	$C_{E,sell}(t)$/($/kWh)
Peak	(11, 15, 19, 21)	0.12	0.10
Intermediate	(8, 10, 16, 18, 22, 23)	0.07	0.06
Valley	(1, 7, 24)	0.03	0.02

Table 3. Parameters of ESS.

Type	$\eta_{E,chh}/\eta_{E,dis}$	τ	μ	$\gamma_{ESS,ch}/\gamma_{ESS,dis}$	SOC_{max}	SOC_{min}	Initial SOC	ESS_{max}/(kWh)
ES	0.9	0.001	/	0.2	1	0.2	0.2	100
HS	0.95	/	0.01	0.25	0.8	0	0.8	100

Table 4. Pollutant emission coefficients and penalty prices.

Type	CO_2	SO_2	NO_x
MT (kg/kWh)	0.202	0.000928	0.000876
Power grid (kg/kWh)	0.272	0.0018	0.0016
District heating network (kg/kWh)	0.889	0.0012	0.0011
Penalty ($/kg)	0.032	2.227	9.445

Table 5. Other parameters.

L_{HV}/(kWh/m^3)	C_{NG}/($/m^3)	$C_{H,buy}(t)$/($/kWh)	$C_{H,sell}(t)$/($/kWh)	η_W	R_{MT}
9.7	0.375	0.018	0.012	0.15	1.08

5.2. Simulation Results Analysis

In order to illustrate the advantages of the presented CHP-based MG system, two scenarios are set up to analyze its economic cost and environmental cost.

Scenario 1: The CHP-based MG system is connected to the district heating network, and heat energy can be exchanged between the CHP-based MG system and the district heating network.

Scenario 2: The CHP-based MG system is not connected to the district heating network, and all the heat load must be balanced by internal components of the CHP-based MG system.

Additionally, three cases under different objective functions are set as follows:

Case 1: The objective function only considers the economic cost.

Case 2: The objective function only considers the environmental cost.

Case 3: The objective function considers both the economic cost and the environmental cost, and the same weighting factors 0.5 are set in TOPSIS method to obtain the optimal decision solution.

5.2.1. Results and Analysis of Scenario 1

The Pareto-optimal solution set of Scenario 1 obtained by the MOBCC algorithm is shown in Figure 5. The economic cost and environmental cost of the three cases are given in Table 6.

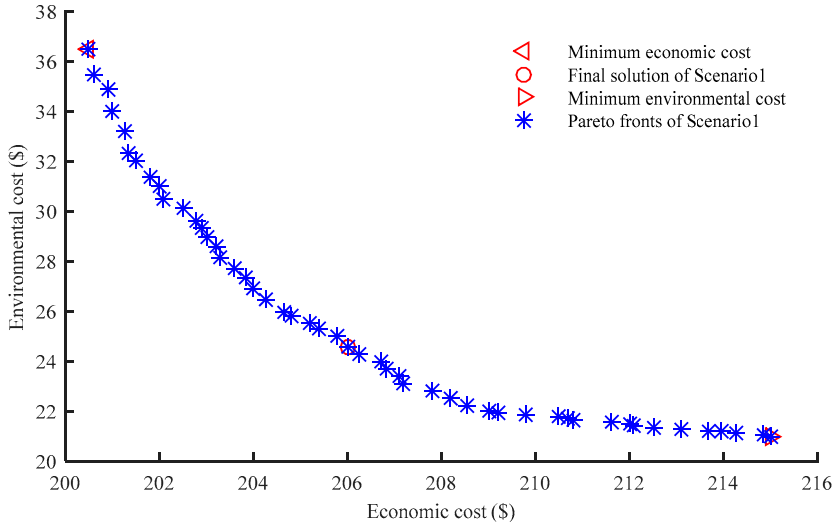

Figure 5. Pareto-optimal solution set of Scenario 1.

Table 6. Costs of three dispatching results.

Type	Economic Cost/$	Environmental Cost/$
Case 1	200.53	36.87
Case 2	214.89	21.69
Case 3	206.12	24.65

It can be seen from Figure 5 and Table 6 that the economic cost of the CHP-based MG system is minimum while the environmental cost is maximum in Case 1. The CHP-based MG system can buy electricity from distribution network and buy heat from district heating network to reduce economic cost. Since the CHP-based MG system prefers to dispatch clean energy or the power generation unit with less pollution, the environmental cost is minimum while the economic cost is maximum in Case 2. Solutions of Case 3 take into account both of the economic cost and environmental cost of the CHP-based MG system, and the dispatch results are the trade-off between Case 1 and Case 2. In the actual scheduling process, the decision maker can set the weight of the two economic and environmental objectives according to the expected preferences, and choose the satisfactory solution from the optimal solution set.

Taking Case 3 in Scenario 1 as an example, more results and analysis are presented as follows:

1. Results and analysis of power outputs and exchanged energy

Assuming that the power outputs of WT and PV are firstly dispatched to meet part of the load, and the remaining electric load and heat load are satisfied by the power outputs of other sources in the CHP-based MG system. The power outputs and the exchanged energy in the CHP-based MG system are shown in Figures 6 and 7.

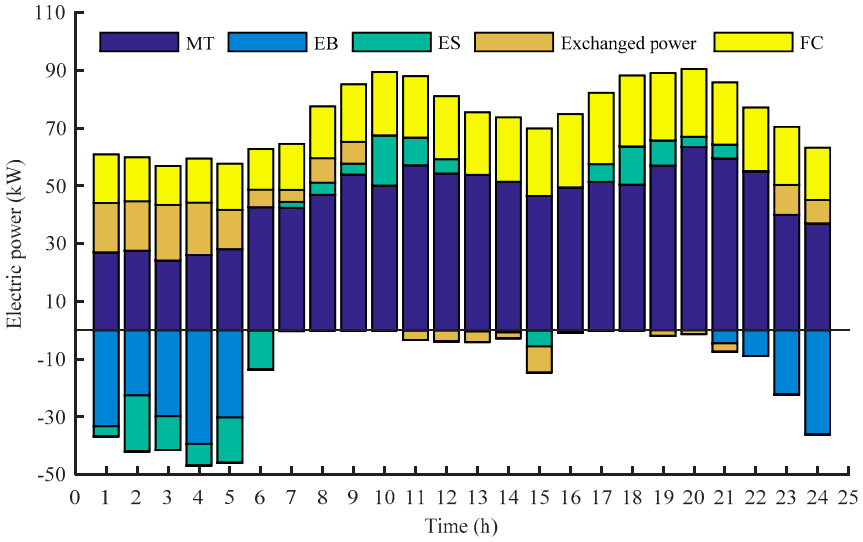

Figure 6. Results of electric power.

Figure 6 shows that the FC (fuel cell) continues to generate electricity during the whole scheduling period. During the electric load valley period, the CHP-based MG system can buy some electricity from the distribution network under low electricity price to reduce the economic cost. However, buying electricity from the distribution network will increase the environmental cost, and thus the amount of purchased electricity is limited. During the electric load peak period, the FC generates more electricity to meet electricity load of the distribution network under high electricity price. At the same time, the excessive electricity can be sold to the distribution network to obtain certain benefits. In the whole scheduling period, the battery is charged during the electric load valley period and discharged at the electric load peak period, which utilizes the price difference to reduce the operational cost of the

CHP-based MG system. The MT (micro-turbine) power generation is mainly to meet the heat load due to its high operation cost. However, when the MT power generation cost is lower than the electricity purchasing cost from the grid, it will generate power to meet the electric load demand.

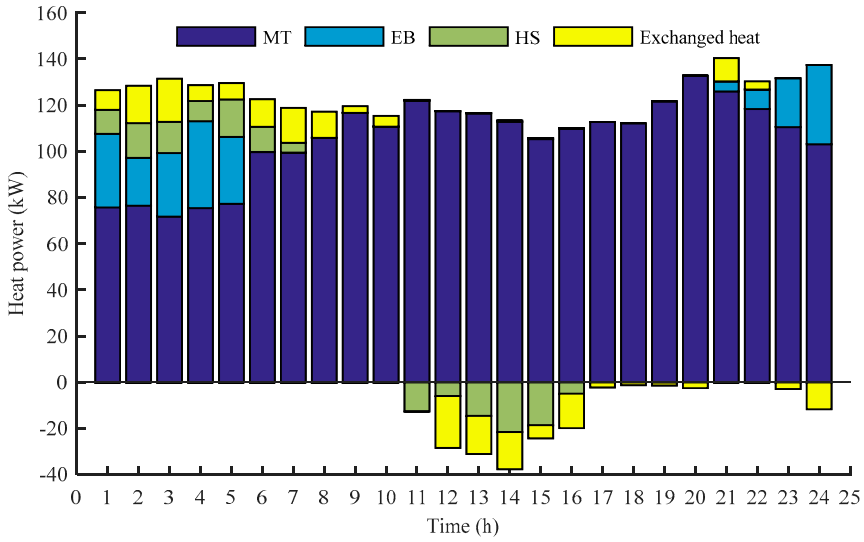

Figure 7. Results of heat power.

There is a certain difference between the peak and valley periods of the electric and heat load. Figure 7 shows that the heat load is mainly satisfied by the CHP unit, because the heat load demand is high at night while it is lower during the day. Moreover, it is observed that the EB (electric boiler) converts electric power to heat and thus supplies some heat load at night. During the period 1:00–7:00, the HS discharges heat to meet heat load so as to reduce the output of the MT. When the output of the MT can meet the electricity load balance, it is not necessary to generate more power to meet the heat load, instead, purchasing some heat from district heating network would be more economic to reduce the total operational cost. However, since purchasing heat from the district heating network will increase the environmental cost, the amount of purchased heat energy will be limited to ensure the total operational and environmental cost minimum. When heat load is low at daytime, the electric load is relatively high, and some excessive heat generated by the CHP unit is stored in HS for future heat load. The remaining excessive heat is sold to the district heating network for profit, which avoids the waste of heat and reduces the cost of the CHP-based MG system.

2. Analysis of wind power consumed by EB

The electric load is low at night while the heat load and the wind power are large, and thus the EB can convert the electricity into heat by consuming the wind power as much as possible. By this way, both the economic cost and environmental cost of the CHP-based MG system are reduced. To further analyze the situation of wind power consumption, consider two subcases of the CHP-based MG system: an MG with an EB, and an MG without any EB. When there is no EB in the CHP-based MG system, the CHP unit has to increase power output to meet the heat load at night, which can result in more than 70 kWh curtailment of wind power, see Figure 8. Therefore, it can be concluded that when there is an EB in the CHP-based MG system, the wind power can be consumed effectively.

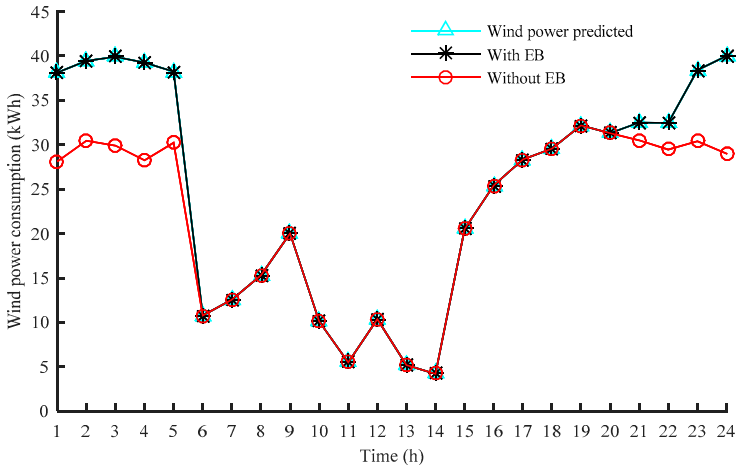

Figure 8. Comparison of wind power utilization.

3. Influence of initial SOC of ESS

The ESS has a bi-directional energy flow, and thus it can shift energy from one time period to another time period to stabilize the load fluctuation. However, the initial SOCs of the energy storage device can affect the operational mode of the CHP-based MG system. Therefore, two subcases are considered to further analyze the influence of initial SOCS of the ESS. In Subcase 1, the initial SOC of HS is the maximum and the initial SOC of ES is the minimum. In Subcase 2, the initial SOC of HS is the minimum and the initial SOC of ES is the minimum. In the scheduling cycle, the SOCs of different ESS in Subcase 1 and Subcase 2 are shown in Figures 9 and 10, respectively.

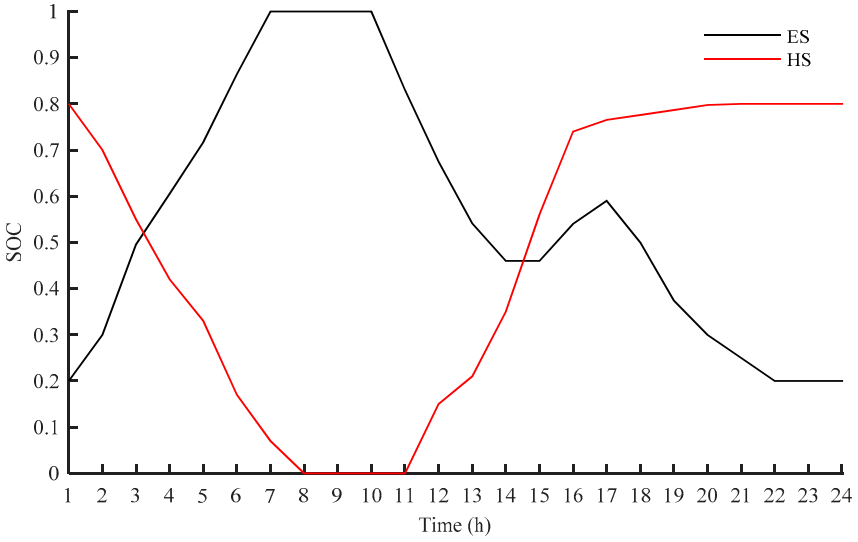

Figure 9. SOCs of ESS in Subcase 1.

From the comparison results between Figures 9 and 10, it can be seen that the ES can coordinate with the HS in Subcase 1. In Subcase 1, the battery is fully charged and the heat storage tank discharges significantly at night, which reduces the CHP unit output. When heat load is small and electricity load are large during the daytime, the HS is charged with heat and the ES discharges electricity. In Subcase 2, Figure 10 shows that the ES cannot complement well the HS due to lower initial SOC of HS. More power output of the CHP unit is used to meet the heat load because the heat load is larger at night. There is no excessive heat to store and the stored electricity of the ES is also decreased. The HS

stores heat after 11:00 a.m. and releases heat after 8:00 p.m. Therefore, as shown in Table 7, both the economic cost and environmental cost of Subcase 1 are lower than those of Subcase 2.

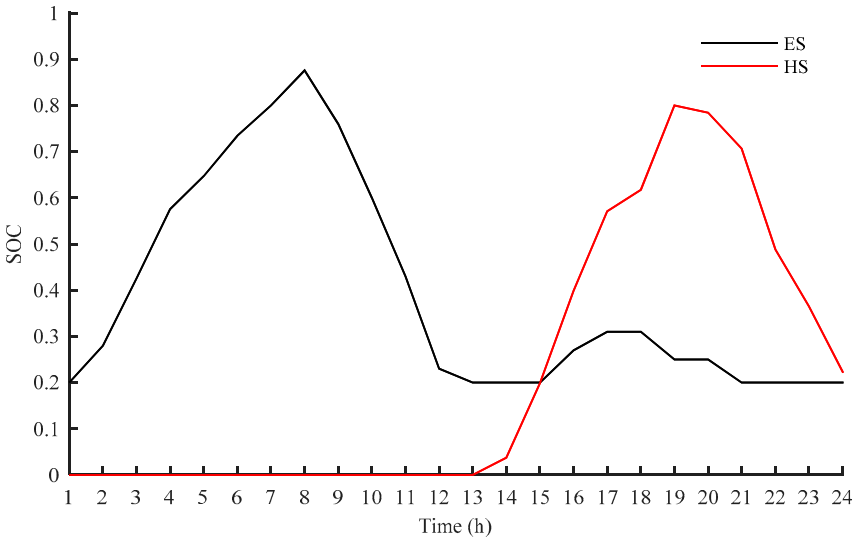

Figure 10. SOCs of ESS in Subcase 2.

Table 7. Cost comparison of two schemes.

Schemes	C_1/$	C_2/$
1	206.12	24.65
2	213.38	27.34

5.2.2. Comparison Analysis of Scenarios 1 and 2

To illustrate the advantages of proposed CHP-based MG system, the Pareto-optimal solution set of Scenario 1 and Scenario 2 obtained by MOBCC algorithm are shown in Figure 11.

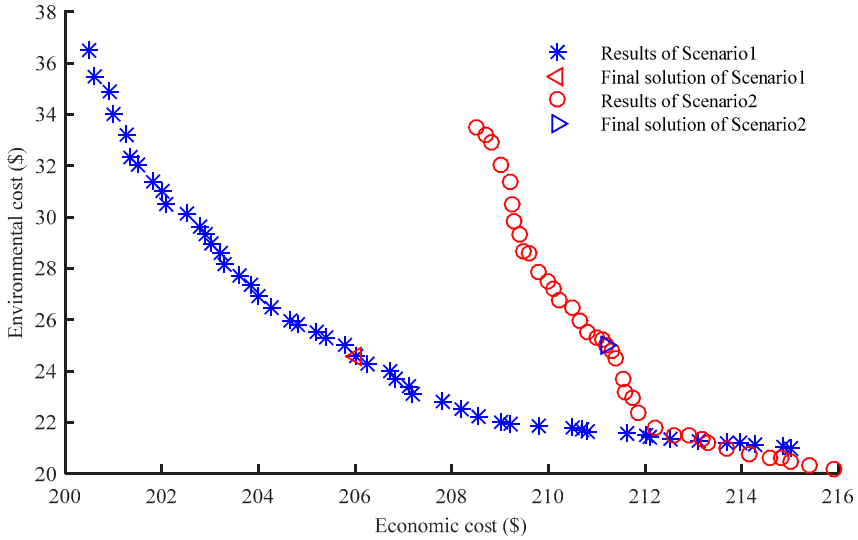

Figure 11. Results of Scenarios 1 and 2.

It can be seen that when the economic cost is less than $213, the economic cost and environmental cost in Scenario 1 are mostly lower than in Scenario 2. However, when the economic cost is more than $213, the economic cost and environmental cost in Scenario 1 are both higher than in Scenario 2.

Therefore, to better compare the CHP-based MG system under the two scenarios, it is important to obtain an equilibrium from the contradictive economic cost and environmental cost.

The final solutions of two scenarios obtained by the TOPSIS method are given in Table 8. It can be seen from Table 8 that better objective values in terms of both the economic cost and the environmental cost are obtained in Scenario 1 than those in Scenario 2. Hence, heat energy exchange between the CHP-based MG system and the district heating network should be encouraged.

Table 8. Cost in two scenarios.

Scenarios	Final Solutions	
	C_1/\$	C_2/\$
1	206.12	24.65
2	211.28	25.23

Optimal results of the CHP-based MG system in Scenario 2 are shown in Figures 12 and 13. Compared to Scenario 2, the CHP-based MG system purchases more electricity from the distribution network in Scenario 1 during the night. Meanwhile, the MG buys part of the heat from district heating network to reduce the output of MT unit because the MT generation cost is higher in the night. During the daytime, to meet the demand of electric load and heat load, the power output of the MT increases in the daytime compared to that at night. Moreover, from Figures 7 and 13, it can be observed that the CHP-based MG system can sell excessive heat of the MT to the district heating network to obtain some income, which can avoid the waste of heat when the heat storage tank is full. Furthermore, from Figures 6 and 12, it is observed that the FC power output is increased in Scenario 2 while it is decreased in Scenario 1. This is because that the increased FC power output in Scenario 2 is used to meet the electric load at the heat load valley period, which can reduce the power output of the MT due to its high operating cost. However, the operational cost in Scenario 1 is even lower, since the heat income is higher than the reduced cost by the FC.

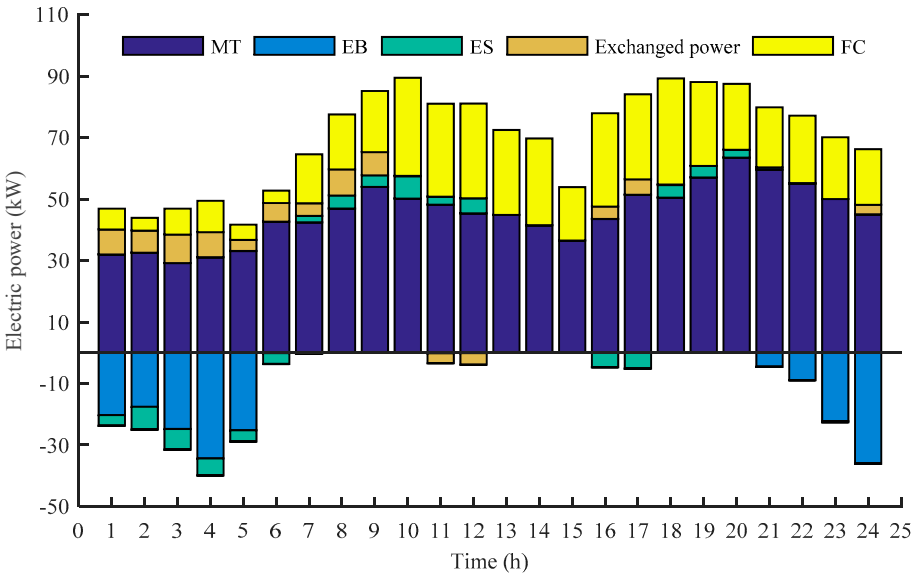

Figure 12. Results of electric power.

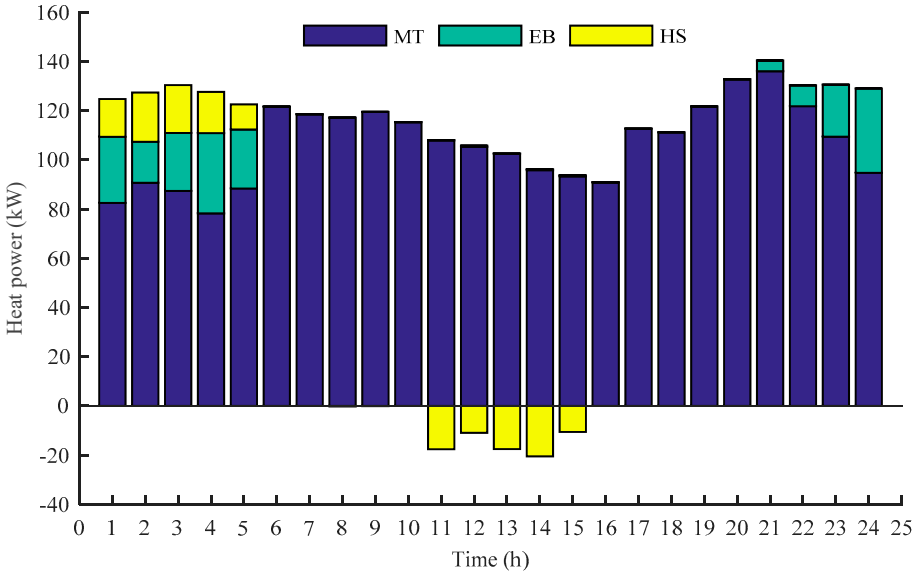

Figure 13. Results of heat power.

6. Conclusions

This paper presents a flexible CHP-based MG system, which is connected to both the electric power distribution network and the district heating network, and thus it can exchange not only electricity with the distribution network but also heat with the district heating network. A multi-objective optimal dispatch model is proposed to consider both of the economic cost and environmental cost. The MOBCC algorithm is utilized to solve this multi-objective scheduling problem, and the TOPSIS method is adopted to choose the final decision solution. Simulation results demonstrate that the flexible CHP-based MG system can improve the economic operation and reduce the pollutant emission simultaneously. The EB can facilitate the wind power utilization, and the initial SOCs of the ESS also have an obvious influence on the economic operation and pollutant emission.

As a future work, we intend to consider the uncertainties for the power outputs of WT and PV, along with the integrated demand response, to enhance the economic and emission operation of the CHP-based MG system.

Author Contributions: All authors contributed equally to the work.

Funding: This research received was funded by National Natural Science Foundation of China (61873225) and (61374098), Provincial Graduate Innovation Assistant Project 2018 (023000307), and National Natural Science Foundation of Hebei Province (F2016203507).

Conflicts of Interest: The authors declare no conflict of interest.

Nomenclature

Abbreviations

CHP	Combined heat and power
FC	Fuel cell
MG	Microgrid
MOBCC	Multi-objective bacterial colony chemotaxis
MT	Micro-turbine
PV	Photovoltaic
SOC	State of charge
TOPSIS	Technique for Order of Preference by Similarity to Ideal Solution
WT	Wind turbine

Constants

$C_{E,buy}(t), C_{E,sell}(t)$	Price of purchasing/sell electricity from/to distribution network at time t
$C_{H,buy}(t), C_{H,sell}(t)$	Price of purchasing/sell heat from/to district heating network at time t
C_k	Penalty price of the pollutant emission k
C_{NG}	Natural gas price
$E_{ESS,max}$	Rated capacity of ESS
L_{HV}	Low calorific value of natural gas
N_T	Scheduling period
$\eta_{ES,ch}, \eta_{ES,dis}$	Charging/discharging efficiency of battery
η_{EB}	Conversion efficiency of electric boiler
$\eta_{HS,ch}, \eta_{HS,dis}$	Heat storage/release efficiency of heat storage tank
η_{HL}	Heat loss rate of micro-turbine
$P_{EXE,max}, P_{EXE,min}$	Maximum/minimum power allowed to exchange with the tie line
$P_L(t), Q_L(t)$	Electrical/heat load of CHP-based MG at time t
$P_{PV}^{max}, P_{WT}^{max}$	Maximum power output of wind turbine/ photovoltaic system
$Q_{EXH,max}, Q_{EXH,min}$	Maximum/minimum heat power from the district heating network
R_{MT}	Heating recovery rate of bromine chiller
$\gamma_{MT,k}, \gamma_{EXE,k}, \gamma_{EXH,k}$	Pollutant emission factor of the micro-turbine, power grid, district heat network
$\gamma_{ESS,ch}, \gamma_{ESS,dis}$	Charge/discharge ratio of ESS
SOC_{max}, SOC_{min}	Maximum/minimum SOC of ESS
Δt	Sampling time period
τ	Self-discharging rate of battery
δ	Heat loss rate of heat energy exchange

Variables

$C_{EXE}(t), C_{EXH}(t)$	Exchanged electricity/heat cost of CHP-based MG system at time t
$C_{FC}(t), C_{MT}(t)$	Fuel cost of fuel cell/micro-turbine at time t
$C_{OM}(t)$	Equipment operation and maintenance cost at time t
$E_{ES}(t), H_{HS}(t)$	Amount of energy remained in the battery/heat storage tank at time t
$E_{ESS}(t)$	Remained energy of ESS at time t
$\eta_{FC}(t), \eta_{MT}(t)$	Power generation efficiency of fuel cell/micro-turbine at time t
$P_{ES,ch}(t), P_{ES,dis}(t)$	Charging/discharging power of battery at time t
$P_{ESS}(t)$	Power of ESS at time t
$P_{ESS,ch}(t), P_{ESS,dis}(t)$	Charging/discharging power of ESS at time t
$P_{EXE}(t), Q_{EXH}(t)$	Exchanged electric/thermal power at time t
$P_{EB}(t), P_{FC}(t), P_{MT}(t)$	Electric power of electric boiler/fuel cell/micro-turbine at time t
$P_{FC}(t), P_{MT}(t), P_{PV}(t), P_{WT}(t)$	Power output of fuel cell/micro-turbine/photovoltaic system/wind turbine at time t
$Q_{EB}(t), Q_{MT}(t), Q_{MT,h}(t)$	Heat power of electric boiler/micro-turbine/bromine chiller at time t
$Q_{HS,ch}(t), Q_{HS,dis}(t)$	Heat power stored/released at time t

References

1. Guo, X.; Zhang, X.; Guan, H.; Kerekes, T.; Blaabjerg, F. Three phase ZVR topology and modulation strategy for transformerless PV system. *IEEE Trans. Power Electron.* **2019**, *34*, 1017–1021. [CrossRef]
2. Guo, X. A novel CH5 inverter for single-phase transformerless photovoltaic system applications. *IEEE Trans. Circ. Syst. II Express Briefs* **2017**, *64*, 1197–1201. [CrossRef]
3. Zhou, K.; Yang, S.; Shao, Z. Energy Internet: The business perspective. *Appl. Energy* **2016**, *178*, 212–222. [CrossRef]
4. Liu, Z.; Chen, Y.; Zhuo, R.; Jia, H. Energy storage capacity optimization for autonomy microgrid considering CHP and EV scheduling. *Appl. Energy* **2018**, *210*, 1113–1125. [CrossRef]
5. Bustos, C.; Watts, D. Novel methodology for microgrids in isolated communities: Electricity cost-coverage trade-off with 3-stage technology mix, dispatch & configuration optimizations. *Appl. Energy* **2017**, *195*, 204–221. [CrossRef]

6. Adam, A.; Fraga, E.S.; Brett, D. Options for residential building services design using fuel cell based micro-CHP and the potential for heat integration. *Appl. Energy* **2015**, *138*, 685–694. [CrossRef]
7. Monteiro, E.; Moreira, N.A.; Ferreira, S. Planning of micro-combined heat and power systems in the Portuguese scenario. *Appl. Energy* **2009**, *86*, 290–298. [CrossRef]
8. Chen, S.X.; Gooi, H.B.; Wang, M.Q. Sizing of Energy Storage for Microgrids. *IEEE Trans. Smart Grid* **2012**, *3*, 142–151. [CrossRef]
9. Yang, Y.; Pei, W.; Qi, Z. Optimal sizing of renewable energy and CHP hybrid energy microgrid system. In Proceedings of the IEEE PES Innovative Smart Grid Technologies, Tianjin, China, 21–24 May 2012; pp. 1–5. [CrossRef]
10. Kopanos, G.M.; Georgiadis, M.C.; Pistikopoulos, E.N. Energy production planning of a network of micro combined heat and power generators. *Appl. Energy* **2013**, *102*, 1522–1534. [CrossRef]
11. Carmen, W.; Eric, S.F.; Adrian, M. A multi-objective framework for cost-unavailability optimisation of residential distributed energy systems design. *Sustain. Energy Grid Netw.* **2017**, *9*, 104–117. [CrossRef]
12. Adam, H.; Yael, P.; Josep, G. Microgrids: A review of technologies, key drivers, and outstanding issues. Renewable and Sustainable Energy Reviews. *Renew. Sustain. Energy Rev.* **2018**, *90*, 402–411. [CrossRef]
13. Anna, S.; Alberto, B.; Nicola, D.; Alberto, M. A model for the optimal design and management of a cogeneration system with energy storage. *Energy Build.* **2016**, *124*, 241–247. [CrossRef]
14. Nicola, D.; Alberto, B.; Anna, S.; Alberto, M. Components design and daily operation optimization of a hybrid system with energy storages. *Energy* **2016**, *117*, 569–577. [CrossRef]
15. Wu, J.; Yan, J.; Jia, H.; Hatziargyriou, N.; Djilali, N.; Sun, H. Integrated Energy Systems. *Appl. Energy* **2016**, *167*, 155–157. [CrossRef]
16. Mark, O.; Ben, K. Energy comes together: The integration of all systems. *IEEE Power Energy Mag.* **2013**, *11*, 18–23. [CrossRef]
17. Jin, M.; Feng, W.; Liu, P.; Marnay, C.; Spanos, C. MOD-DR: Microgrid optimal dispatch with demand response. *Appl. Energy* **2017**, *187*, 758–776. [CrossRef]
18. Anvari-Moghaddam, A.; Rahimi-Kian, A.; Mirian, M.S.; Guerrero, J.M. A multi-agent based energy management solution for integrated buildings and microgrid system. *Appl. Energy* **2017**, *203*, 41–56. [CrossRef]
19. Ma, L.; Liu, N.; Zhang, J.; Tushar, W.; Yuen, C. Energy Management for Joint Operation of CHP and PV Prosumers Inside a Grid-Connected Microgrid: A Game Theoretic Approach. *IEEE Trans. Ind. Inform.* **2016**, *12*, 1930–1942. [CrossRef]
20. Pan, Z.; Guo, Q.; Sun, H. Feasible region method based integrated heat and electricity dispatch considering building thermal inertia. *Appl. Energy* **2016**, *192*, 395–407. [CrossRef]
21. Silvente, J.; Kopanos, G.M.; Pistikopoulos, E.N.; Espuña, A. A rolling horizon optimization framework for the simultaneous energy supply and demand planning in microgrids. *Appl. Energy* **2015**, *155*, 485–501. [CrossRef]
22. Martinez-Ceseña, E.A.; Good, N.; Syrri, A.L.; Mancarella, P. Techno-economic and business case assessment of multi-energy microgrids with co-optimization of energy, reserve and reliability services. *Appl. Energy* **2018**, *210*, 896–913. [CrossRef]
23. Nazari-Heris, M.; Abapour, S.; Mohammadi-Ivatloo, B. Optimal Economic Dispatch of FC-CHP based Heat and Power Micro-grids. *Appl. Therm. Eng.* **2017**, *114*, 756–769. [CrossRef]
24. Li, M.; Zhang, X.; Li, G.; Jiang, C. A feasibility study of microgrids for reducing energy use and GHG emissions in an industrial application. *Appl. Energy* **2016**, *176*, 138–148. [CrossRef]
25. Aluisio, B.; Dicorato, M.; Forte, G.; Trovato, M. An optimization procedure for Microgrid day-ahead operation in the presence of CHP facilities. *Sustain. Energy Grid Netw.* **2017**, *11*, 34–45. [CrossRef]
26. Niknam, T.; Golestaneh, F. Probabilistic multiobjective operation management of microgrids with hydrogen storage and polymer exchange fuel cell power plants. *Fuel Cells* **2012**, *12*, 809–826. [CrossRef]
27. Lu, Z.; Zhao, H.; Xiao, H.; Wang, H.; Wang, H. An improved multi-objective bacteria colony chemotaxis algorithm and convergence analysis. *Appl. Soft Comput.* **2015**, *31*, 274–292. [CrossRef]
28. Lu, Z.; He, S.; Feng, T.; Li, X.; Guo, X.; Sun, X. Robust economic/emission dispatch considering wind power uncertainties and flexible operation of carbon capture and storage. *Int. J. Electr. Power Energy Syst.* **2014**, *63*, 285–292. [CrossRef]

29. Lu, Z.; Feng, T.; Li, X. Low-carbon emission/ economic power dispatch using the multi-objective bacterial colony chemotaxis optimization algorithm considering carbon capture power plant. *Int. J. Electr. Power Energy Syst.* **2013**, *53*, 106–112. [CrossRef]
30. Olson, D.L. Comparison of Weights in TOPSIS Models. *Math. Comput. Model.* **2004**, *40*, 721–727. [CrossRef]
31. Wu, X.; Wang, X.; Wang, J.; Bie, Z. Economic Generation Scheduling of a Microgrid using Mixed integer programming. *Proc. CSEE* **2013**, *33*, 1–8. [CrossRef]
32. Li, Z.; Xu, Y. Optimal coordinated energy dispatch of a multi-energy microgrid in grid-connected and islanded modes. *Appl. Energy* **2018**, *210*, 974–986. [CrossRef]
33. Gianfreda, A.; Grossi, L. Zonal price analysis of the Italian wholesale electricity market. In Proceedings of the 2009 6th International Conference on the European Energy Market, Leuven, Belgium, 27–29 May 2009; pp. 1–6. [CrossRef]